Neuro-Oncology Advances

4(1), 1–10, 2022 | https://doi.org/10.1093/noajnl/vdac023 | Advance Access date 21 February 2022

Noninvasive differentiation of molecular subtypes of adult nonenhancing glioma using MRI perfusion and diffusion parameters

Ilanah J. Pruis†, Stephan R. Koene†, Sebastian R. van der Voort, Fatih Incekara, Arnaud J. P. E. Vincent, Martin J. van den Bent, Geert J. Lycklama à Nijeholt, Rishi D. S. Nandoe Tewarie, Sophie E. M. Veldhuijzen van Zanten, and Marion Smits

Department of Radiology and Nuclear Medicine, Erasmus MC, Rotterdam, The Netherlands (I.J.P., S.R.K., S.R.V., F.I., S.E.M.V.Z., M.S.); Department of Neurosurgery, Erasmus MC, Rotterdam, The Netherlands (A.J.P.E.V.); Department of Neurology, Erasmus MC, Rotterdam, The Netherlands (M.J.B.); Department of Radiology and Nuclear Medicine, Haaglanden MC, Den Haag, The Netherlands (G.J.L.N.); Department of Neurosurgery, Haaglanden MC, Den Haag, The Netherlands (R.D.S.N.T.)

†These authors shared the first authorship of this work.

Corresponding Author: Marion Smits, MD, PhD, Department of Radiology and Nuclear Medicine, Erasmus MC, Dr. Molewaterplein 40, 3015 GD Rotterdam, The Netherlands (marion.smits@erasmusmc.nl).

Abstract

Background. Nonenhancing glioma typically have a favorable outcome, but approximately 19–44% have a highly aggressive course due to a glioblastoma genetic profile. The aim of this retrospective study is to use physiological MRI parameters of both perfusion and diffusion to distinguish the molecular profiles of glioma without enhancement at presentation.

Methods. Ninety-nine patients with nonenhancing glioma were included, in whom molecular status (including 1p/19q codeletion status and IDH mutation) and preoperative MRI (T2w/FLAIR, dynamic susceptibility-weighted, and diffusion-weighted imaging) were available. Tumors were segmented semiautomatically using ITK-SNAP to derive whole tumor histograms of relative Cerebral Blood Volume (rCBV) and Apparent Diffusion Coefficient (ADC). Tumors were divided into three clinically relevant molecular profiles: IDH mutation (IDHmt) with ($n = 40$) or without ($n = 41$) 1p/19q codeletion, and ($n = 18$) IDH-wildtype (IDHwt). ANOVA, Kruskal-Wallis, and Chi-Square analyses were performed using SPSS.

Results. rCBV (mean, median, 75th and 85th percentile) and ADC (mean, median, 15th and 25th percentile) showed significant differences across molecular profiles ($P < .01$). Posthoc analyses revealed that IDHwt and IDHmt 1p/19q codeleted tumors showed significantly higher rCBV compared to IDHmt 1p/19q intact tumors: mean rCBV (mean, SD) 1.46 (0.59) and 1.35 (0.39) versus 1.08 (0.31), $P < .05$. Also, IDHwt tumors showed significantly lower ADC compared to IDHmt 1p/19q codeleted and IDHmt 1p/19q intact tumors: mean ADC (mean, SD) 1.13 (0.23) versus 1.27 (0.15) and 1.45 (0.20), $P < .001$).

Conclusions. A combination of low ADC and high rCBV, reflecting high cellularity and high perfusion respectively, separates IDHwt from in particular IDHmt 1p/19q intact glioma.

Key Points

- Perfusion is higher in IDHwt and IDHmt 1p/19q codeleted than IDHmt 1p/19q intact nonenhancing glioma.
- Diffusion is significantly lower in IDHwt versus IDHmt nonenhancing glioma.

Importance of the Study

Nonenhancing glioma is a difficult entity because, despite their relatively benign radiological appearance, 19–44% of these tumors are of the glioblastoma-like genetic profile with an aggressive course and poor outcome. Noninvasive tools to differentiate the molecular profiles of nonenhancing glioma are thus of great value to anticipate their clinical course and to aid treatment decision making. We are the first to specifically focus on a patient population selected on the basis of presurgical radiological tumor appearance, allowing a real-world assessment of the potential value of perfusion and diffusion MRI in a patient presenting with a nonenhancing lesion. Based on a higher rCBV, IDHwt tumors could be differentiated from IDHmt 1p/19q intact tumors, but not from IDHmt 1p/19q codeleted tumors. ADC however, was lower in IDHwt than in all IDHmt tumors, with or without 1p/19q codeletion.

Although glioma have a low incidence (5.9:100 000), they induce the highest loss of life years compared to other cancer types.[1] At presentation, approximately 9% of high-grade glioma and 48% of low-grade glioma do not show enhancement on MRI after contrast agent administration.[2] This is problematic, because—while the majority of these nonenhancing tumors are indeed low-grade and less aggressive—19–44% have a highly aggressive course due to a high-grade like or a so-called glioblastoma genetic profile, requiring rapid intervention.[3,4] Therefore, information even prior to surgery about the molecular profile (i.e. possible presence of a glioblastoma genetic profile) of in particular asymptomatic patients with nonenhancing glioma, can contribute to better-informed treatment decision making.

Noninvasive physiological tissue MRI parameters are promising tools to this end, in particular relative cerebral blood volume (rCBV) and the apparent diffusion coefficient (ADC), representing perfusion and cellularity of an area of interest, respectively.[5–7] It is hypothesized that the rCBV and ADC could serve as surrogate diagnostic markers of tumor grade and aggressiveness to differentiate between molecular profiles.[8–11] In adult glioma, three molecular profiles have been identified based on the isocitrate dehydrogenase (IDH) type 1 or 2 mutation (IDHmt) and the 1p/19q codeletion.[12] These molecular profiles are considered to be fundamental for predicting the clinical disease course and defining treatment. The IDH mutation (>70%) and 1p/19q codeletion (30%) occur most frequently in low-grade glioma, and correlate with better patient survival.[11,13–15] The IDH wildtype (IDHwt), or aggressive molecular profile, is typically found in glioblastoma.[13]

Previous studies using physiological MRI parameters found a significantly higher rCBV and lower ADC in IDHwt compared to IDHmt tumors.[9,10] Likewise, an inverse correlation between rCBV and ADC with tumor grade was found, showing high rCBV and low ADC in high-grade tumors, reflecting high vascularity and cellularity, respectively.[16] Also, a higher rCBV in 1p/19q codeleted tumors compared to 1p/19q intact tumors was found, presumably related to their known differences in vascularization.[8,11] None of the previous studies, however, investigated the biological correlation of both parameters in the whole spectrum of molecular profiles *and* in the setting of initially nonenhancing lesions. In this study, we aim to combine physiological MRI parameters of both perfusion and diffusion to distinguish the molecular profiles in a large group of patients presenting with a nonenhancing lesion. We, therefore, hypothesize that rCBV increases and that ADC decreases along the spectrum from IDHmt 1p/19q intact to IDHmt 1p/19q codeleted to IDHwt tumors.

Materials and Methods

Patients

Internal review board approval for this study was obtained from the Medical Ethics Committee at Erasmus MC. Due to the retrospective nature of the study, informed consent was waived. Patients with nonenhancing glioma who underwent surgery between June 2011 and January 2018 in Erasmus MC, University Medical Centre Rotterdam, The Netherlands or Haaglanden Medical Centre (HMC), The Hague, The Netherlands were considered for inclusion in this retrospective study. A nonenhancing tumor was defined as: patients who presented with a nonenhancing lesion who were selected for surgery and had histopathologically confirmed glioma. Inclusion criteria were: age ≥ 18 years, known molecular status for 1p/19q codeletion and IDH mutation according to the WHO 2016 classification and the recent cIMPACT-NOW 3 update,[17] and preoperative MR imaging available including at least T2w/FLAIR, dynamic susceptibility-weighted (DSC) and diffusion-weighted (DWI) images. Any information initially missing of patients included in the dataset, was retrieved retrospectively. At the time of analyses no data was missing.

Tissue Sequence Analyses

Tumor tissue was analyzed via immunohistochemistry and for most tumors also Ion Torrent Next-Generation Sequencing (NGS) was performed to determine the following genes and SNPs in all patients: (i) hotspot mutation sites: IDH1 codon 132, IDH2 codon 40 and 172, and (ii) LOH analysis using SNPs for 1p, 19q, chromosome 7 (including the EGFR locus) and chromosome 10. TERT promoter mutations were determined in some patients by NGS, in some with SNaPshot assay for the 2 hotspot mutations in glioma (C22bT and C250T). Tumors were divided into three groups

based on their molecular profile: (i) IDHmt with 1p/19q codeletion, (ii) IDHmt without 1p/19q codeletion, and (iii) IDHwt (without 1p/19q codeletion). Tumors with an IDHwt molecular profile were further characterized, when NGS was available, for the presence or absence of molecular features of glioblastoma (EGFR amplification, TERT mutation, and/or chromosome 7/10 aberrations).

Image Acquisition

Imaging parameters according to clinical imaging protocols and scanners at each institution are described in Table 1. All imaging series (conventional MR, DSC, and DW-images) were acquired with either a 1.5 or 3T superconducting system (General Electric® (GE) or Siemens®).

At Erasmus MC, Gadovist® (gadobutrol 1 mmol/ml, Bayer AG, Berlin, Germany) was used as contrast agent. A preload contrast dosage of 0.05 ml/kg was used and the remainder of a 15 ml Gadovist® bolus injection during DSC acquisition with a flowrate of 5 ml/s. At HMC, Dotarem® (Gadoterate meglumine 0.5 mmol/ml, Guerbet, Aulnay-sous-Bois, France) was used as a contrast agent. A preload dosage of 10 ml was used and a 20 ml Dotarem® bolus injection during DSC acquisition with a flowrate of 4 ml/s.

Image Processing

T2w/FLAIR series were used for tumor localization, and loaded into ITK-SNAP version 3.6.0 (University of Pennsylvania and Utah, USA)[18] for tumor segmentation and to calculate tumor volumes semiautomatically with the active contour-classification-segmentation method. This segmentation was visually inspected and manually corrected by an independent researcher (S.K, I.P or F.I) if needed. Laterality and location of the tumor were determined by visual inspection.

Table 1. MRI Acquisition Parameters for Each Participating Hospital

Hospital	Erasmus MC[a]	HMC[b]	HMC[b]
N	76	14	9
Manufacturer	GE	Siemens	Siemens
Field strength (T)	1.5 or 3	1.5	1.5
T2w/FLAIR	**3D FLAIR**	**2D T2w**	**2D T2w**
Matrix	512 × 512	440 × 512	224 × 256
TR (ms)	8400	2500	3200
TE (ms)	120	356	379
TI (ms)	2100	-	-
FA (°)	90	180	120
Slice thickness (mm)	0.8	1.2	1
Perfusion (DSC)			
Matrix	128 × 128	256 × 224	128 × 128
Contrast agent	Gadovist®[c]	Dotarem®[d]	Dotarem®[d]
Dosage (ml)	15 (including preload)	30 (including preload)	30 (including preload)
Preload	Yes: 0.05 ml/kg	Yes: 10 ml	Yes: 10 ml
Flowrate (ml/sec)	5	4	4
TR (ms)	2000	2400	1490
TE (ms)	45	46	30
FA (°)	90	70	90
Slice thickness (mm)	5 or 6	5 or 6	5 or 6
Diffusion (DWI)			
Matrix	256 × 256	256 × 256	192 × 192
TR (ms)	8000	3600	3200
TE (ms)	80	100	89
Slice thickness (mm)	3 or 5	5	5
b-values (s/mm^2)	0 and 1000	0, 500, and 1000	0, 500, and 1000

DSC, Dynamic Susceptibility Contrast; DWI, Diffusion-Weighted Imaging; FA, Flip Angle; TE, Echo Time; TI, Inversion Time; TR, Repetition Time.
[a]Erasmus Medical Centre University, Rotterdam, The Netherlands;
[b]Haaglanden Medical Centre, Den Haag, The Netherlands;
[c]Gadobutrol 1 mmol/ml (Bayer AG, Berlin, Germany);
[d]Gadoterate meglumine 0.5 mmol/ml (Guerbet, Aulnay-sous-Bois, France).

Raw DSC and DWI DICOM-series were loaded into OsiriX Lite 9.0® (Pixmeo, Bernex, Switzerland) and visually examined on quality and artifacts.

The rCBV maps were generated using the OsiriX-plugin IB-Neuro™ (Imaging Biometrics, Elm Grove, USA). Three regions of interest (ROI) were automatically placed on arterial structures within the brain for estimating the Arterial Input Function (AIF). All scans included the required minimum number of baseline volumes ($n = 4$) and time-points ($n = 30$). In case the AIF was found to be insufficient upon visual inspection, the scans were excluded from this study ($n = 4$). Standardized leakage corrected rCBV maps were computed based on Voxel Intensity Standardized™ signal values.

The ADC maps were generated using the OsiriX-plugin IB-Diffusion™ (Imaging Biometrics, Elm Grove, USA). Volumes with b-values b = 0 and b = 1000 s/mm^2 were used for two-point ADC calculation (ADC = ln(S0/ S1)/ (b1 – b0)). In case more baseline volumes with other b-values were available, those volumes were not included in the calculation of the ADC maps.

The standardized leakage corrected rCBV maps and the ADC maps were exported in raw DICOM format. The T2w/FLAIR scans were registered to the rCBV and ADC maps, and the tumor segmentations were transformed according to the resulting parameters. All registrations were individually verified. Failed registrations were re-analyzed and recreated. Histograms were obtained within the tumor segmentation from which mean, median, and percentile rCBV and ADC values were derived for each patient.

Statistical Analysis

Statistical analysis was performed with Statistical Package for the Social Sciences (SPSS) version 24.0.0.1. (IBM Corporation, New York, USA).

Normality of the data was determined using Kolmogorov-Smirnov Z-test for continuous variables (age, tumor volume, rCBV, and ADC) and reported by mean and standard deviation (SD) for normally distributed variables and by median and interquartile range (IQR) for non-normally distributed variables, respectively. For categorical variables (sex, grade, laterality, and location of tumor), frequencies and percentages were reported. The Analysis of Variance test (ANOVA) or independent T-test and the Kruskal-Wallis test (KW) or Mann-Whitney U test were used for normally and non-normally distributed variables, respectively. The F-ratio was used and the Brown-Forsythe and Welch's F-ratio were reported instead when the assumption of homogeneity of variances was violated (Levene's test). For categorical data, the Chi-Square test was used and Fisher's exact test was reported instead when the minimum count in a variable was < 5. A P-value < .05 was considered a statistically significant difference.

The included patients were compared with the excluded patients for the available baseline characteristics. The rCBV and ADC parameters were first compared between hospitals and between scanning protocols to assess their potential influence on the data. The duration (in months) between first lesion detection and surgical resection or biopsy was also assessed. As a baseline characterization of the samples, the three molecular profile groups were analyzed for sex, age, volume, grade, laterality, and location of the tumor. The three molecular profile groups were then compared for perfusion and diffusion using the calculated rCBV and ADC maps respectively. The mean, median, 75th, and 85th percentile rCBV and the mean, median, 15th, and 25th percentile ADC values were compared between groups. We used percentile values derived from the histogram analysis rather than the minimum and maximum values as the latter are heavily dependent on outliers. The aforementioned inverse correlation between rCBV and ADC[16] was analyzed in our dataset using a Pearson's Chi-square test and the median rCBV/ADC ratio was compared across molecular profile groups. Posthoc analyses with pairwise comparisons were performed when a significant correlation was found using Bonferroni corrected p-value for multiple testing (three pairwise comparisons). The accuracy of the median rCBV/ADC ratio to differentiate molecular profiles was also determined using receiver operating characteristics (ROC) analysis. The areas under the ROC curve (AUCs) with 95% confidence intervals (CI) were calculated and optimal cutoffs with sensitivity and specificity were reported. All analyses were repeated in the selection of IDHwt tumors with confirmed glioblastoma-like features based on NGS.

Results

Patients

From the 342 patients with nonenhancing lesions a total of 99 patients were eligible and included in the main analysis (Figure 1). The main reason for exclusion was the lack of DWI and/or DSC data. Patient and tumor characteristics are shown in Table 2. We found that the excluded patients were slightly younger than the included patients ($P = .011$), however, this did not influence the distribution of molecular profiles (i.e. 21% versus 18.2% of IDHwt tumors) indicating that the sample is a good representation of the domain of all patients with a nonenhancing glioma. Mean patient age was 47 years and the majority of patients were male (64%). Tumors were most frequently located in the frontal lobe (42%). Eighteen tumors were IDHwt.

Age ($P = .200$), mean rCBV ($P = .050$), 85th percentile rCBV ($P = .071$) and mean ($P = .114$), median ($P = .200$), 15th percentile ($P = .200$) and 25th percentile ($P = .200$) ADC were normally distributed. Median ($P < .001$) and 75th percentile ($P = .039$) rCBV and tumor volume ($P < .001$) were non-normally distributed. The inverse correlation between the median rCBV and median ADC was confirmed (r = –0.608; $P < .001$). The ratio variable was non-normally distributed ($P < .001$). The rCBV and ADC parameters did not significantly differ between Erasmus MC and HMC ($P > .1$). There was no influence of the scanning protocol on the rCBV and ADC parameters ($P > .1$). The median (IQR) duration between lesion detection and surgery was 3.0 (9.0) months and was significantly longer in IDHmt 1p/19q codeleted tumors (4.4 (21.0) months) compared to IDHwt tumors (2.0 (2.0) months) ($P = .013$), which was not explained by a difference in age ($P = .906$).

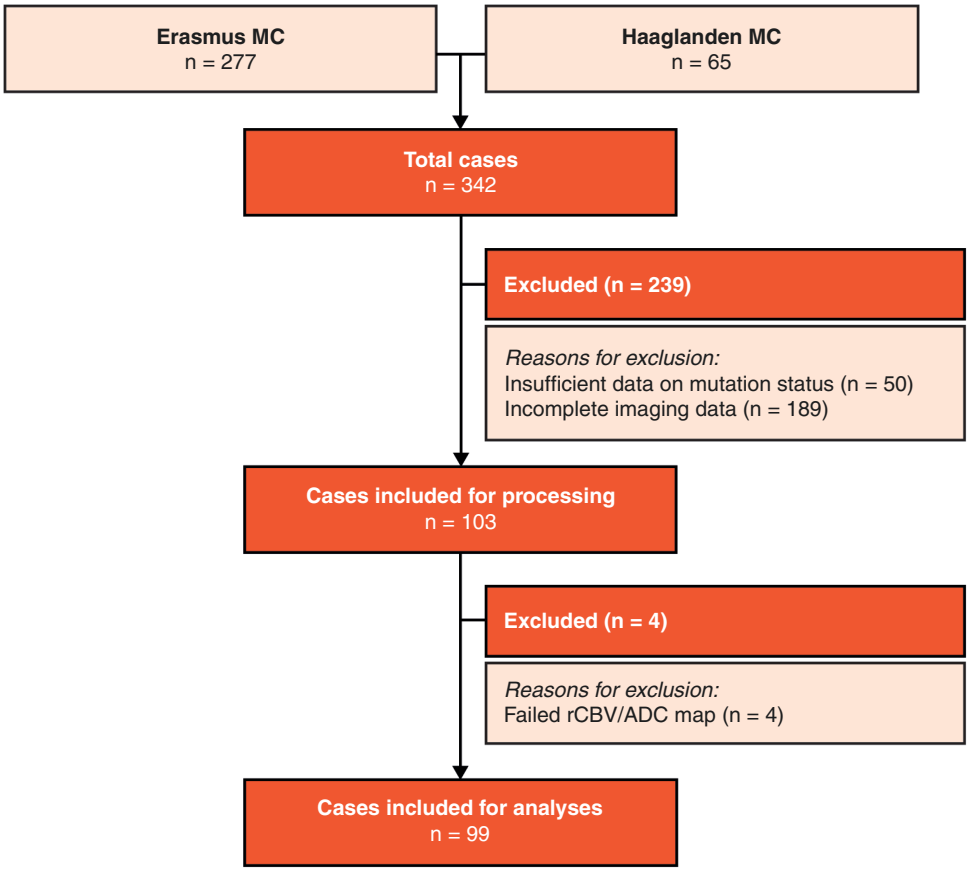

Figure 1. Flow-chart of the study.

Baseline Characterization of the Molecular Profiles

No statistically significant difference in sex (P = .493), volume (P = .223) or brain hemisphere (P = .287) of the tumor was found across the molecular profiles. Age was significantly different across molecular profiles (P < .001). Pairwise comparison revealed that patients with IDHwt tumors were significantly older than patients with IDHmt 1p/19q codeleted tumors (P = .002) and IDHmt 1p/19q intact tumors (P < .001). Tumor grade was different across molecular profiles albeit borderline significant (P = .047) and no significant correlations were revealed with pairwise comparisons. Tumor lobe involvement was significantly different across molecular profiles for the frontal lobe (P = .001), temporal lobe (P = .012) and basal ganglia (P = .005). Pairwise comparison revealed that (i) IDHmt 1p/19q codeleted tumors were significantly more often located in the frontal lobe compared to IDHwt tumors (P < .001) and (ii) IDHmt 1p/19q codeleted tumors were significantly less often located in the temporal lobe than IDHmt 1p/19q intact (P = .015) and IDHwt (P = .009) tumors. Basal ganglia involvement was significant across molecular profiles but no multiple testing corrected significant correlations were found with pairwise comparisons (P < .0167).

MR Perfusion and Diffusion of Molecular Profiles

The rCBV and ADC parameters separated by molecular profile are displayed in Table 3. Comparison of the three molecular profiles showed significant differences for all rCBV and ADC values (P < .01) (Figure 2).

Pairwise comparison of the rCBV parameters showed that (i) IDHwt tumors had significantly higher values compared to IDHmt 1p/19q intact tumors for mean (P = .003), median (P = .001), 75th percentile (P = .003) and 85th percentile (P = .005) rCBV, and (ii) IDHmt 1p/19q codeleted tumors had significantly higher values compared to IDHmt 1p/19q intact tumors for mean (P = .001), median (P < .001) and 75th percentile (P = .011) rCBV. No significant differences were found for rCBV parameters between IDHwt tumors and IDHmt 1p/19q codeleted tumors (P > .05).

Pairwise comparison of ADC parameters revealed significantly lower values in IDHwt tumors compared to both (i) IDHmt 1p/19q codeleted tumors for mean (P = .029) and median (P = .020) ADC, and (ii) IDHmt 1p/19q intact tumors for mean (P < .001), median (P < .001), 15th percentile (P = .004) and 25th percentile (P < .001) ADC. IDHmt 1p/19q codeleted tumors had significantly lower ADC values than IDHmt 1p/19q intact tumors for mean (P < .001), median (P < .001) and 25th percentile (P = .005) ADC.

Table 2. Patient and Tumor Characteristics Separated by Molecular Profile

	Total ($n = 99$)	IDHmt 1p/19q codeletion ($n = 40$)	IDHmt 1p/19q intact ($n = 41$)	IDHwt ($n = 18$)	*P*-value
Sex, *n* (%)					.493[a]
Male	63 (63.6)	23 (57.5)	29 (70.7)	11 (61.1)	
Female	36 (36.4)	17 (42.5)	12 (29.3)	7 (38.9)	
Mean age, years (SD)	47.07 (14.84)	47.33 (12.86)	40.85 (14.12)	60.67 (11.53)	<.001[b]
Median tumor volume, cm^3 [IQR]	43.64 [22.19–92.17]	38.33 [15.05–70.06]	56.81 [33.58–105.67]	37.51 [16.42–77.87]	.223[c]
Tumor grade, *n* (%)					.047[d]
II	78 (78.8)	35 (87.5)	32 (78.0)	11 (61.1)	
III	17 (17.2)	5 (12.5)	8 (19.5)	4 (22.2)	
IV	4 (4.0)	-	1 (2.4)	3 (16.7)	
Tumor hemisphere, *n* (%)					.287[d]
Left	45 (45.5)	22 (55.0)	14 (34.1)	9 (50.0)	
Right	48 (48.5)	15 (37.5)	25 (61.0)	8 (44.4)	
Bilateral	6 (6.1)	3 (7.5)	2 (4.9)	1 (5.6)	
Tumor lobe involvement, *n* (%)					
Frontal	62 (62.6)	32 (80.0)	25 (61.0)	5 (27.8)	.001[a]
Parietal	22 (22.2)	8 (20.0)	9 (22.0)	5 (27.8)	.773[d]
Occipital	1 (1.0)	-	1 (2.4)	-	1.000[d]
Temporal	31 (31.3)	6 (15.0)	16 (39.0)	9 (50.0)	.012[a]
Basal Ganglia	3 (3.0)	-	-	3 (16.7)	.005[d]
Insula	22 (22.2)	5 (12.5)	11 (26.8)	6 (33.3)	.115[d]

IDH, isocitrate dehydrogenase; mt, mutated; wt, wildtype.
[a]Pearson's Chi Square;
[b]One-way ANOVA test;
[c]Kruskal-Wallis test;
[d]Fisher's Exact test.

A significant correlation was found between molecular profile and the median rCBV/ADC ratio (KW(2) = 29.548, $P < .001$), which was highest in IDHwt tumors followed by IDHmt 1p/19q codeleted tumors and lowest in IDHmt 1p/19q intact tumors (Figure 3). The median rCBV/ADC ratio was significantly higher in (i) IDHwt tumors compared to IDHmt 1p/19q intact tumors ($P < .001$) and in (ii) IDHmt 1p/19q codeleted tumors compared to IDHmt 1p/19q intact tumors ($P < .001$).

The optimal combination of sensitivity (80%) and specificity (73%) was found at a threshold of 0.56 for the median rCBV/ADC ratio to discriminate IDHmt 1p/19q codeleted tumors from IDHmt 1p/19q intact tumors. The AUC was 0.80 (95% CI: 0.71–0.90). The optimal combination of sensitivity (72%) and specificity (55%) was found at a threshold of 0.80 to discriminate IDHmt 1p/19q codeleted tumors from IDHwt tumors. The AUC was 0.65 (95% CI: 0.48–0.82). The optimal combination of sensitivity (83%) and specificity (83%) was found at a threshold of 0.63 to discriminate IDHmt 1p/19q intact tumors from IDHwt tumors. The AUC was 0.84 (95% CI: 0.70–0.97).

Secondary Analysis in the Selection of IDHwt Tumors with Confirmed Glioblastoma-Like Features

We confirmed by NGS that the majority of the IDHwt tumors were of the glioblastoma genetic profile (EGFR amplification, TERT mutation, and/or chromosome 7/10 aberrations; $n = 12/18$). For 6/18 IDHwt tumors (histopathologically diagnosed as presumed glioblastoma in $n = 5$ and low-grade in $n = 1$) NGS data was insufficient or missing. We repeated the analyses including only the IDHwt tumors with confirmed molecular glioblastoma-like features, which yielded similar findings (Supplementary Table 1). However, multiple pairwise comparisons lost significance which may be explained by a lack of statistical power. For IDHwt tumors versus IDHmt 1p/19q codeleted tumors the significant differences disappeared for: temporal lobe involvement of the tumor, mean and median ADC. For IDHwt tumors versus IDHmt 1p/19q intact tumors the significant differences disappeared for the rCBV parameters. The median rCBV/ADC ratio remained significantly higher in IDHwt tumors and in IDHmt 1p/19q codeleted tumors compared to IDHmt 1p/19q intact tumors.

Table 3. The rCBV and ADC Parameters Separated by Molecular Profile

	IDHmt 1p/19q codeleted (n = 40)	IDHmt 1p/19q intact (n = 41)	IDHwt (n = 18)	P-value
rCBV parameters				
Mean	1.35 (0.39)	1.08 (0.31)	1.46 (0.59)	.001[a]
Median	0.92 [0.79–1.05]	0.71 [0.58–0.83]	0.94 [0.80–1.46]	<.001[b]
75th percentile	1.54 [1.23–1.85]	1.25 [1.01–1.47]	1.66 [1.43–2.22]	.001[b]
85th percentile	2.10 (0.67)	1.77 (0.55)	2.38 (0.91)	.004[a]
ADC parameters				
Mean	1.27 (0.15)	1.45 (0.20)	1.13 (0.23)	<.001[a]
Median	1.25 (0.16)	1.47 (0.23)	1.08 (0.24)	<.001[a]
15th percentile	1.00 (0.14)	1.08 (0.17)	0.92 (0.20)	.003[a]
25th percentile	1.08 (0.14)	1.21 (0.18)	0.98 (0.22)	<.001[a]
Median rCBV/ADC ratio				
Median	0.78 [0.58–0.92]	0.50 [0.36–0.60]	0.94 [0.66–1.32]	<.001[b]

ADC, apparent diffusion coefficient; IDH, isocitrate dehydrogenase; mt, mutated; rCBV, relative cerebral blood volume; wt, wildtype.
Data are displayed in mean (SD) and median [IQR] for normally and non-normally distributed parameters, respectively. rCBV parameters are expressed in arbitrary units (IB Neuro™, Imaging Biometrics, Elm Grove, USA). ADC parameters are expressed in 10 mm^2/s.
[a]One-way ANOVA test;
[b]Kruskal-Wallis test.

Discussion

This is the first and largest quantitative study using combined physiological MR parameters in which we demonstrate that perfusion and diffusion parameters are different between molecular profiles in nonenhancing glioma and may thus inform clinical decision making. Significantly higher rCBV and lower ADC values were found in IDHwt tumors compared to IDHmt 1p/19q intact tumors. While there was no significant difference in rCBV between IDHwt and IDHmt 1p/19q codeleted tumors, these tumors did show differences in ADC, being lower in IDHwt glioma.

Our findings regarding perfusion are in correspondence with previous research.[8–11,19] It was previously demonstrated that IDHwt versus IDHmt tumors correlated with higher activity of the gene *HIF1A*.[9] This gene, which encodes a subunit of the hypoxia-inducible transcription factor 1, facilitates vasculo- and angiogenesis providing a direct link between genotype, tumor biology, and increased perfusion. In addition, the well-known microvascular proliferation in even low-grade 1p/19q codeleted tumors might explain their increased perfusion compared to 1p/19q intact tumors.[11,20] Most studies also included enhancing glioma in their analyses which might explain the higher values of rCBV and ADC found in comparison with our study.[8,11,19,21]

We know from literature, that the value of diffusion parameters to distinguish molecular profiles in glioma is less clear.[8,10,21,22] Fellah et al. (2013) did not find any significant differences in ADC between molecular profiles.[8] However, Leu et al. (2017) found a significantly lower ADC in IDHwt tumors compared to IDHmt tumors in general—and specifically in IDHmt 1p/19q intact tumors.[10] In addition, lower ADC has been reported in 1p/19q codeleted tumors compared to 1p/19q intact tumors.[21,22] These findings are in line with our findings of low ADC in IDHwt tumors, higher ADC in IDHmt 1p/19q codeleted tumors, and highest ADC in IDHmt 1p/19q intact tumors. We further confirm the inverse correlation between the median rCBV and ADC.[16] This finding also corresponds with the underlying tumor biology of increased vascularity of tumor cells and thus increased blood volume on the one hand and increased cellularity due to higher proliferation rates and thus decreased free water motion on the other hand.[6,7,23]

While ADC was lower on average in IDHwt compared with IDHmt 1p/19q codeleted tumors, we did not find a statistically significant difference in the 15th and 25th percentile ADC between these types of tumors. This might be explained by a larger heterogeneity in ADC values in IDHwt tumors compared to the other two profiles. The ADC findings in the IDHwt molecular profile group are likely not influenced by other rare tumors (e.g. pleomorphic xanthoastrocytoma or ganglioglioma) as we confirmed the majority of IDHwt tumors were of the glioblastoma genetic profile.[24] The larger heterogeneity in rCBV and ADC values in IDHwt tumors could also be explained by the relatively small sample of IDHwt tumors (n = 18) in our study cohort. The smaller sample of IDHwt tumors is inherent to the low incidence of nonenhancing glioma with this molecular profile.[25,26] A further explanation may be that, while the lower ADC values in themselves are similar between IDHwt and IDHmt 1p/19q codeleted tumors, a larger fraction of IDHwt tumors has lower ADC values, thus resulting in an overall lower ADC than the other tumor types.

Our AUC findings are similar to previous studies, i.e. between 0.7 and 0.9.[9,10,19,21,27] Our results indicate that determining a cutoff value based on (a combination of) the

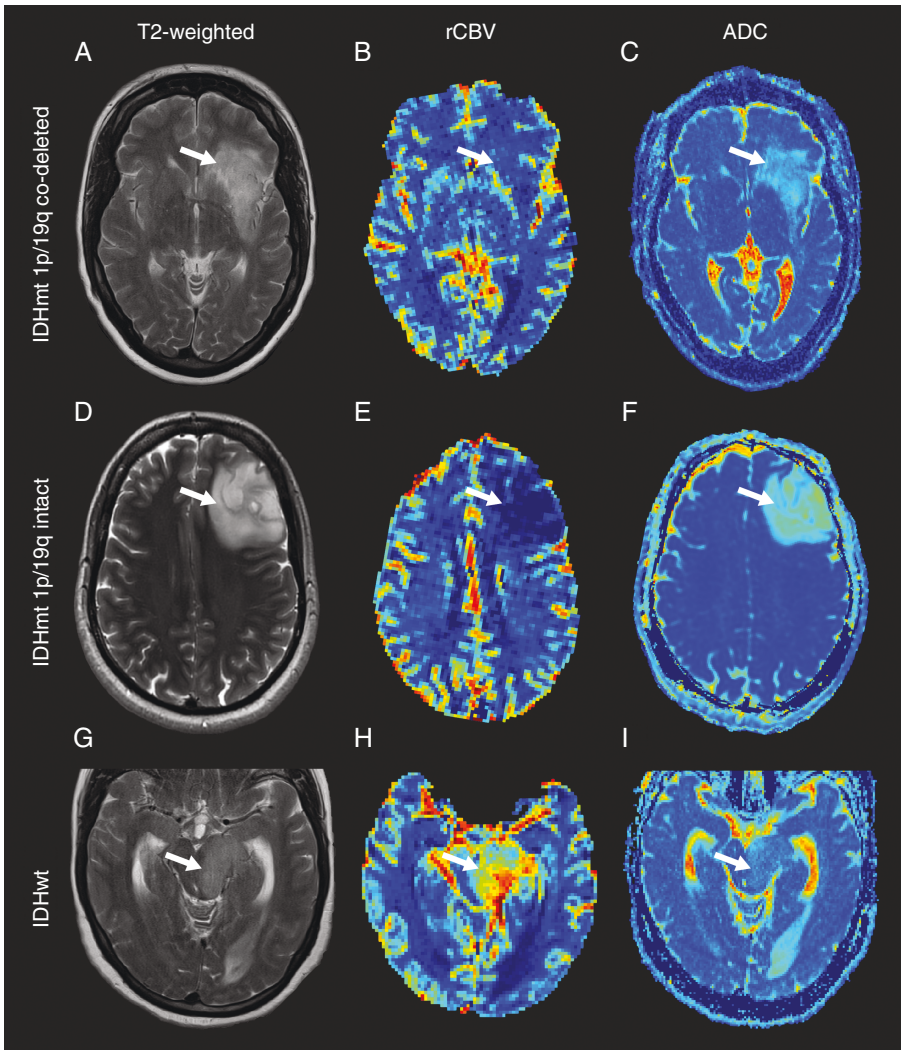

Figure 2. Brain images of IDHmt 1p/19q codeleted (A–C), IDHmt 1p/19q intact (D–F) and IDHwt (G–I) nonenhancing glioma. T2-weighted (A, D, G) images are shown with the corresponding standardized leakage corrected rCBV colormap and ADC colormap showing intermediate rCBV (B) and intermediate ADC (C) for IDHmt 1p/19 codeleted glioma, low rCBV (E) and high ADC (F) for IDHmt 1p/19q intact glioma and high rCBV (H) and low ADC (I) for IDHwt glioma at the location of the tumor (white arrows).

rCBV and ADC might help to distinguish molecular profiles of nonenhancing glioma in the future. However, our findings need further validation in an independent validation cohort.

The significant differences found in the baseline characteristics, i.e. patients' age and tumor grade as well as localization, of each of the different molecular profiles are not surprising.[8,16,20,28–31] The higher male/female ratio across molecular profiles in our study can be explained by the general difference in incidence of adult glioma in the population.[32] We could not replicate the significantly higher tumor volumes in IDHmt versus IDHwt tumors found previously.[10] This is most likely due to the fact that enhancing tumors, which are commonly larger, were not included in our study. The tumor volume differences in 1p/19q codeleted versus 1p/19q intact tumors might additionally be explained by possible differences in the relative contribution of nontumor, i.e. vasogenic edemia, to the T2/FLAIR hyperintense signal used for volume calculation.

A major strength of our study regards minimization of inter- and intra-observer variability by full segmentation of tumor tissue instead of manual placement of regions of interest.[8,10,11,19] In addition, segmentation was done semiautomatically, and standardized leakage corrected rCBV maps were calculated automatically using IB-Neuro, further reducing user-related variability.[33] For future research it would be interesting to also include more than 2 b-values in the ADC analyses to diminish the effect of small vessel perfusion.[27]

This study also had some limitations. First, there were some differences in scanning protocols due to the multicenter origin of the data. Although it is generally known that perfusion imaging is highly site and user specific (e.g. different imaging parameters, contrast agent and

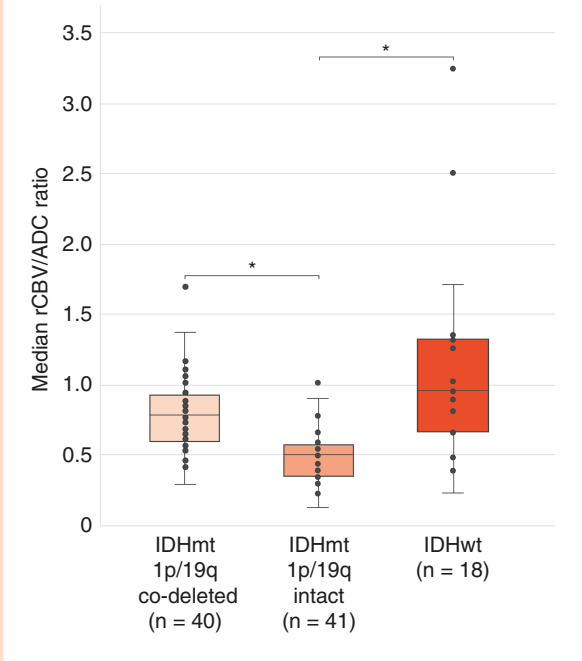

Figure 3. Boxplots of the median rCBV/ADC ratio separated by molecular profile, *$P < .001$.

bolus injection)[5]—the rCBV and ADC values in our study did not differ significantly across scanning protocols nor varied dependent on the hospital of inclusion. Moreover, the quality control, postprocessing, and statistical analyses were all performed in the same center (Erasmus MC) preventing any variabilities due to data processing differences between centers. Thus, the differences in scanning protocols probably did not have a substantial impact on the findings. Second, the retrospective nature of this study demands supplementary investigation of the predictive value of rCBV and ADC in a prospective cohort. We do however think that this heterogeneity of the data represents the continuous, real life clinical setting. Also, for applicability in a real life prospective clinical setting it should be taken into account that other diagnoses (i.e. glioneuronal grade 1 lesions) might also present with nonenhancing lesions. Nonetheless, we believe our study represents the population of adult patients presenting with a nonenhancing lesion as best as was possible.

It is also important to note that our findings—even though statistically significant—are only valid at the group level, and cannot be directly applied to the individual patient. The differences in physiological parameters between IDHwt and IDHmt 1p/19q codeleted tumors in particular were small, only showing a difference in ADC and not in rCBV. However, we know that 1p/19q codeleted tumors have other distinct MRI characteristics such as and indistinct tumor margin, calcifications, extensive cortical involvement, and inhomogeneity of T2-weighted signal intensity.[34,35] Combining MR parameters such as rCBV and ADC in a prediction model with other patient characteristics (e.g. age and tumor location) would be a logical next step, but our study population was not powered for this. Using such a model may further improve the noninvasive classification and enable differentiation at the individual patient level. This has previously been studied,[8,10,36] but comparison of the parameters significantly contributing to these models is difficult due to differences in the research question and data analysis and the heterogeneity between study populations. In addition, apart from the model of Chawla et al. (2013), who used a leave-one-out cross-validation test,[36] these models are not validated and demand confirmation in an independent validation cohort. We therefore should be cautious with direct translation of such a model to the clinic.

In conclusion, this study showed that in nonenhancing glioma the physiological MR parameters rCBV and ADC can—at the group level—help to distinguish molecular profiles—and in particular IDHwt. Future prospective studies are required to validate these findings at the individual patient level, to evaluate their potential to anticipate the patient's clinical course and aid decision making in clinical practice prior to surgery—with possible improvements of accuracy through including additional patient characteristics such as age and tumor location.

Supplementary material

Supplemental material is available at *Neuro-Oncology Advances* online.

Keywords

ADC | MRI | molecular profile | nonenhancing glioma | rCBV

Acknowledgments

The authors thank Imaging Biometrics, Elm Grove, for providing a research license of the software for data analysis.

Funding

This work was financially supported by Semmy Foundation (Stichting Semmy) to I.J.P. and by the Dutch Cancer Society (KWF project number EMCR 2015-7859) to S.R.V. and F.I.

Conflict of interest statement. The authors declare no potential conflicts of interest

Authorship statement. Study concept and design: M.S. Analysis of data: I.J.P., S.R.K. and S.R.V. Writing of the manuscript: I.J.P., S.R.K., S.R.V., and M.S. Intellectual contribution and revision of the manuscript: I.J.P., S.R.K., S.R.V., F.I., A.J.P.E.V., M.J.B., G.J.L.N., R.D.S.N.T., S.E.M.V.Z., M.S.

References

1. Rouse C, Gittleman H, Ostrom QT, Kruchko C, Barnholtz-Sloan JS. Years of potential life lost for brain and CNS tumors relative to other cancers in adults in the United States, 2010. *Neuro Oncol* 2016;18(1):70–77.
2. Scott JN, Brasher PM, Sevick RJ, Rewcastle NB, Forsyth PA. How often are nonenhancing supratentorial gliomas malignant? A population study. *Neurology* 2002;59(6):947–949.
3. Eichberg DG, Di L, Morell AA, et al. Incidence of high grade gliomas presenting as radiographically non-enhancing lesions: experience in 111 surgically treated non-enhancing gliomas with tissue diagnosis. *J Neurooncol.* 2020;147(3):671–679.
4. Kudulaiti N, Zhang H, Qiu T, et al. The Relationship Between IDH1 mutation status and metabolic imaging in nonenhancing supratentorial diffuse gliomas: A (11)C-MET PET study. *Mol Imaging.* 2019;18:1536012119894087.
5. Petrella JR, Provenzale JM. MR perfusion imaging of the brain: techniques and applications. *AJR Am J Roentgenol.* 2000;175(1):207–19.
6. Eidel O, Neumann JO, Burth S, et al. Automatic analysis of cellularity in glioblastoma and correlation with ADC using trajectory analysis and automatic nuclei counting. *PLoS One.* 2016;11(7):e0160250.
7. Hayashida Y, Hirai T, Morishita S, et al. Diffusion-weighted imaging of metastatic brain tumors: comparison with histologic type and tumor cellularity. *AJNR Am J Neuroradiol.* 2006;27(7):1419–1425.
8. Fellah S, Caudal D, De Paula AM, et al. Multimodal MR imaging (diffusion, perfusion, and spectroscopy): is it possible to distinguish oligodendroglial tumor grade and 1p/19q codeletion in the pretherapeutic diagnosis? *AJNR Am J Neuroradiol.* 2013;34(7):1326–1333.
9. Kickingereder P, Sahm F, Radbruch A, et al. IDH mutation status is associated with a distinct hypoxia/angiogenesis transcriptome signature which is non-invasively predictable with rCBV imaging in human glioma. *Sci Rep.* 2015;5:16238.
10. Leu K, Ott GA, Lai A, et al. Perfusion and diffusion MRI signatures in histologic and genetic subtypes of WHO grade II-III diffuse gliomas. *J Neurooncol.* 2017;134(1):177–188.
11. Jenkinson MD, Smith TS, Joyce KA, et al. Cerebral blood volume, genotype and chemosensitivity in oligodendroglial tumours. *Neuroradiology* 2006;48(10):703–713.
12. Louis DN, Perry A, Wesseling P, et al. The 2021 WHO Classification of Tumors of the Central Nervous System: a summary. *Neuro Oncol* 2021;23(8):1231–1251.
13. Cancer Genome ARN, Brat DJ, Verhaak RG, et al. Comprehensive, integrative genomic analysis of diffuse lower-grade gliomas. *N Engl J Med.* 2015;372(26):2481–2498.
14. Yan H, Parsons DW, Jin G, et al. IDH1 and IDH2 mutations in gliomas. *N Engl J Med.* 2009;360(8):765–773.
15. van den Bent MJ, Brandes AA, Taphoorn MJ, et al. Adjuvant procarbazine, lomustine, and vincristine chemotherapy in newly diagnosed anaplastic oligodendroglioma: long-term follow-up of EORTC brain tumor group study 26951. *J Clin Oncol.* 2013;31(3):344–350.
16. Saberi M, Faeghi F, Ghanaati H, et al. Grading of glioma tumors by analysis of minimum apparent diffusion coefficient and maximum relative cerebral blood volume. *Casp J Neurol Sci* 2016;2(4):42–53.
17. Brat DJ, Aldape K, Colman H, et al. cIMPACT-NOW update 3: recommended diagnostic criteria for "Diffuse astrocytic glioma, IDH-wildtype, with molecular features of glioblastoma, WHO grade IV". *Acta Neuropathol.* 2018;136(5):805–810.
18. Yushkevich PA, Piven J, Hazlett HC, et al. User-guided 3D active contour segmentation of anatomical structures: significantly improved efficiency and reliability. *NeuroImage* 2006;31(3):1116–1128.
19. Tan W, Xiong J, Huang W, et al. Noninvasively detecting Isocitrate dehydrogenase 1 gene status in astrocytoma by dynamic susceptibility contrast MRI. *J Magn Reson Imaging.* 2017;45(2):492–499.
20. Smits M, van den Bent MJ. Imaging correlates of adult glioma genotypes. *Radiology* 2017;284(2):316–331.
21. Cui Y, Ma L, Chen X, et al. Lower apparent diffusion coefficients indicate distinct prognosis in low-grade and high-grade glioma. *J Neurooncol.* 2014;119(2):377–385.
22. Jenkinson MD, Smith TS, Brodbelt AR, et al. Apparent diffusion coefficients in oligodendroglial tumors characterized by genotype. *J Magn Reson Imaging.* 2007;26(6):1405–1412.
23. Baldock AL, Yagle K, Born DE, et al. Invasion and proliferation kinetics in enhancing gliomas predict IDH1 mutation status. *Neuro Oncol* 2014;16(6):779–786.
24. van den Bent MJ, Weller M, Wen PY, et al. clinical perspective on the 2016 WHO brain tumor classification and routine molecular diagnostics. *Neuro Oncol* 2017;19(5):614–624.
25. Wang YY, Wang K, Li SW, et al. Patterns of tumor contrast enhancement predict the prognosis of anaplastic gliomas with IDH1 mutation. *AJNR Am J Neuroradiol.* 2015;36(11):2023–2029.
26. Hempel JM, Brendle C, Bender B, et al. Contrast enhancement predicting survival in integrated molecular subtypes of diffuse glioma: an observational cohort study. *J Neurooncol.* 2018;139(2):373–381.
27. Gihr GA, Horvath-Rizea D, Hekeler E, et al. Histogram analysis of diffusion weighted imaging in low-grade gliomas: in vivo characterization of tumor architecture and corresponding neuropathology. *Front Oncol.* 2020;10:206.
28. Eckel-Passow JE, Lachance DH, Molinaro AM, et al. Glioma groups based on 1p/19q, IDH, and TERT promoter mutations in tumors. *N Engl J Med.* 2015;372(26):2499–2508.
29. Li MY, Wang YY, Cai JQ, et al. Isocitrate dehydrogenase 1 gene mutation is associated with prognosis in clinical low-grade gliomas. *PLoS One.* 2015;10(6):e0130872.
30. Reyes-Botero G, Dehais C, Idbaih A, et al. Contrast enhancement in 1p/19q-codeleted anaplastic oligodendrogliomas is associated with 9p loss, genomic instability, and angiogenic gene expression. *Neuro Oncol* 2014;16(5):662–670.
31. De Leeuw BI, Van Baarsen KM, Snijders TJ, Robe P. Interrelationships between molecular subtype, anatomical location, and extent of resection in diffuse glioma: a systematic review and meta-analysis. *Neurooncol Adv* 2019;1(1):vdz032.
32. Dubrow R, Darefsky AS. Demographic variation in incidence of adult glioma by subtype, United States, 1992-2007. *BMC Cancer* 2011;11:325.
33. Bedekar D, Jensen T, Schmainda KM. Standardization of relative cerebral blood volume (rCBV) image maps for ease of both inter- and intrapatient comparisons. *Magn Reson Med.* 2010;64(3):907–913.
34. Smits M. Imaging of oligodendroglioma. *Br J Radiol.* 2016;89(1060):20150857.
35. van den Bent MJ, Smits M, Kros JM, Chang SM. Diffuse infiltrating oligodendroglioma and astrocytoma. *J Clin Oncol.* 2017;35(21):2394–2401.
36. Chawla S, Krejza J, Vossough A, et al. Differentiation between oligodendroglioma genotypes using dynamic susceptibility contrast perfusion-weighted imaging and proton MR spectroscopy. *AJNR Am J Neuroradiol.* 2013;34(8):1542–1549.